



Watershed infarcts in a multiple microembolic model of monkey

Takakuni Maki^a, Hideaki Wakita^b, Mitsuhito Mase^c, Iori Itagaki^d, Naoyuki Saito^d, Fumiko Ono^d, Kayo Adachi^b, Hidefumi Ito^a, Ryosuke Takahashi^a, Masafumi Ihara^{a,*}, Hidekazu Tomimoto^{e,**}

^a Department of Neurology, Graduate School of Medicine, Kyoto University, Shogoin, Sakyo-ku, Kyoto 606-8507, Japan

^b Department of Vascular Dementia Research, National Institute for Longevity Sciences, National Center for Geriatrics and Gerontology, Japan

^c Department of Neurosurgery and Restorative Neuroscience, Graduate School of Medical Sciences, Nagoya City University, Japan

^d The Corporation for Production and Research of Laboratory Primates, Japan

^e Department of Neurology, Graduate School of Medicine, Mie University, Japan

ARTICLE INFO

Article history:

Received 10 March 2011

Received in revised form 27 April 2011

Accepted 16 May 2011

Keywords:

Watershed infarct

Embolic

Hemodynamic

Macaque monkey

ABSTRACT

It has long been debated whether watershed infarcts are caused by hemodynamic or embolic mechanisms. In the present study, we investigated microembolic roles in the pathogenesis of watershed infarcts by examining MRI in a macaque monkey model of multiple microinfarcts. 50 μ m microbeads were injected into each internal carotid artery twice with a month interval. Monkeys ($n=4$) injected with 2250–2800 microbeads per unilateral side showed both cortical and internal watershed infarcts in the acute phase and atrophic changes with microbleeds in the chronic phase. These results suggest embolic pathogenesis can contribute to the genesis of both cortical and internal watershed infarcts in primates.

© 2011 Elsevier Ireland Ltd. All rights reserved.

Cerebral watershed infarcts are classified as cortical watershed (CWS) and internal watershed (IWS) infarcts – also termed external and internal border-zone infarcts, respectively. The former are generated in the areas between the cortical territories of the anterior cerebral artery (ACA), middle cerebral artery (MCA), and posterior cerebral artery (PCA), while the latter are located in the white matter along and slightly above the lateral ventricle, between the deep and the superficial arterial systems of the MCA, or between the superficial systems of the MCA and ACA [11].

Though neuropathological and physiological studies have shown that either or both hemodynamic and embolic mechanisms principally underlie watershed infarcts, the precise pathogenesis is still a matter of debate. The role of hemodynamic compromise in watershed infarct formation has been well described [9,13,19] and confirmed by experimental studies with primates [1]. Caplan et al. have postulated the coexistence of hypoperfusion and intra-arterial embolism in patients with watershed infarcts and carotid artery disease. They suggested that hemodynamic compromise and microembolism collaborate in the pathogenesis of border-

zone infarcts, meaning that reduced perfusion limits the ability of the bloodstream to wash out emboli, particularly within the border-zone [2]. In addition, evidence of the role of embolism in the pathophysiology of watershed infarcts has been documented using: 1, embolic materials within watershed infarct areas in an autopsy series [10]; 2, induction by glass microspheres in the brains of cadavers [14]; 3, the detection of intra-arterial emboli by transcranial Doppler monitoring in patients with watershed infarcts [17]. Recently Moustafa et al. have reported that IWS infarcts result from microembolism secondary to plaque inflammation [12]. However, direct evidence of microembolic watershed infarcts complemented by experimental studies with primates has been, so far, scarce.

The purpose of the present study is to elucidate the microembolic roles in the pathophysiology of watershed infarcts by examining MRI in a macaque monkey model of multiple microinfarcts; 50 μ m microbeads were thus injected into each internal carotid artery twice with a month interval. In a previous study, macaque monkeys injected with approximately 1400 microbeads were reported to develop multiple lacunar infarcts in the territory of perforating artery on T2-weighted images and a transient decrease in cerebral motor pathway fractional anisotropy on diffusion tensor images [3]. However, the present study revealed that the injection of relatively more microbeads (approximately 2250–2800) resulted in multiple infarcts in the both cortical and internal watershed territories with subsequent brain atrophy on T1-weighted, T2-weighted, and fluid-attenuated inversion recovery (FLAIR) images. Furthermore, we found the development

Abbreviations: ACA, anterior cerebral artery; CCA, common carotid artery; CWS, cortical watershed; FLAIR, fluid-attenuated inversion recovery; ICA, internal carotid artery; IWS, internal watershed; MCA, middle cerebral artery; PCA, posterior cerebral artery.

** Co-Corresponding author. Tel.: +81 75 751 3766; fax: +81 75 751 3766.

* Tel.: +81 59 231 5107; fax: +81 59 231 5082.

E-mail addresses: ihara@kuhp.kyoto-u.ac.jp (M. Ihara), tomimoto@clin.medic.mie-u.ac.jp (H. Tomimoto).

Table 1
MRI analysis results.

Monkey	Number of microbeads	Number of CWS (day 10)	Number of IWS (day 10)	% Tissue loss (day 71)	Number of microbleeds (day 71)
#1	2250	7	8	15.1	8
#2	2250	2	3	7.9	3
#3	2250	1	3	7.0	1
#4	2800	4	6	12.4	5

of microbleeds, which were demonstrated on T2 star-weighted images. Primates possess an evolutionally expanded white matter volume; this may explain why many neuroprotective drugs targeted against neuronal cell death in the gray matter, such as glutamate antagonists and antioxidants, have shown promise in rodent stroke models but have failed to provide efficacy in clinical trials [16]. Therefore, such temporal profiles of MRI images in this primate model may serve to shed light on the mechanisms involved in the embolic stroke and offer possible treatment strategies for brain damage associated with embolic watershed infarcts in humans.

The data reported in the present study were obtained from eight adult male cynomolgus monkeys (*Macaca fascicularis*) of 6–10 years of age, and weighing 4.3–5.4 kg at the first operation. Two monkeys were used for optimizing the experimental conditions, four for obtaining the principal data, and two as intact controls. The monkeys were reared at the Tsukuba Primate Research Center, National Institute of Biomedical Innovation. This study was conducted according to the Rules for Animal Care and Management of the Tsukuba Primate Research Center [7], the Guiding Principles for Animal Experiments Using Nonhuman Primates [Primate Society of Japan, 1986], and the Guide for the Care and Use of Laboratory Animals [National Research Council, 1996]. Protocols of experimental procedures were approved by the Animal Welfare and Animal Care Committee of National Institute of Biomedical Innovation (Osaka, Japan).

We developed a multiple microinfarct model in the macaque monkey as previously described in detail [3,15]. Before surgery, monkeys were anesthetized with isoflurane following sedation with an intramuscular injection of ketamine hydrochloride (Ketalar®, 10 mg/kg; Daiichi-Sankyo Co., Ltd.). From a transfemoral approach, a 4Fr sheath was placed, followed by a guiding catheter (Selecon PA catheter; Clinical Supply) placement into the common carotid artery (CCA). A 1.7Fr microcatheter (Excelsior SL-10; Boston Scientific) was then introduced into the internal carotid artery (ICA) through the guiding catheter. Small particles (Sephacryl; Sigma) of 25–75 μ m diameter (average 50 μ m) suspended in contrast medium/saline were injected into the ICA. The approximate number of particles injected was 330–2800 per unilateral side (660–5600 in total). As an injection of more than 2800 microbeads into the bilateral ICA at the same time will lead to death, due to massive brain edema on the bilateral side, we injected the particles into each ICA twice with a month interval. If the interval of microbeads injection is less than one month, incomplete recovery from the first injection can lead to death, while if the interval is more than two months, the recovery phase is too long to evaluate progressive stroke. Control monkeys underwent the same surgical procedure but were injected with 0.9% saline instead of microbeads.

MRI was performed using the 3T MRI system (MAGNETOM Allegra; Siemens). T1-weighted images, T2-weighted images, T2 star-weighted images and fluid-attenuated inversion recovery (FLAIR) images were obtained before the operation, as well as 3 h and 10, 28, 37, 42, and 71 days after surgery. The imaging protocol consisted of T1-weighted spin echo (repetition time/echo time = 2500/3.89 ms), T2-weighted spin echo (repetition time/echo time = 4000/18 ms), T2 star-weighted spin echo (repetition time/echo time = 612/18 ms) and FLAIR (repetition time/echo

time = 9000/101 ms, inversion time = 2150 ms) imaging series. The slice thickness was 2 mm, and the intersection gap was 2 mm. Location of brain slice was fitted at the anterior commissure (AC) as a guide. To calculate the percentage of brain tissue loss, five serial 2-mm thick coronal sections (2 mm gap) between AC –8 mm and +8 mm were evaluated using Adobe Photoshop (version 7, Adobe System). The brain tissue area in each slice \times distance between slices (4 mm) was summed to approximate the brain tissue volume. Cerebral ischemic lesions were classified into three categories, as previously described [4]: 1, perforating artery infarcts; 2, IWS infarcts; 3, cortical infarcts (either territorial or watershed). IWS infarcts were defined as multiple or confluent lesions located between the deep and superficial arterial systems of the MCA or between the superficial arterial systems of the MCA and the ACA. CWS infarcts were defined as wedge-shaped, corticosubcortical lesions in the anterior border zone between the territory of the ACA and the MCA or in the posterior border zone between the territory of the MCA and the PCA. The CWS regions are boundary zones where functional anastomoses between the two arterial systems exist. FLAIR images were used to distinguish infarcts from dilated perivascular spaces.

We initially varied the number of particles injected from 330 to 2800 per unilateral side (660–5600 in total). Multiple microinfarcts in the acute and chronic phase, and atrophic changes with microbleeds in the chronic phase were observed in parallel with the increased number of particles. In particular, the monkeys injected with more than 2000 per unilateral side (2250, monkey #1–3; 2800, monkey #4) showed both CWS and IWS infarcts besides perforating artery infarcts which were observed in the monkeys injected with 1300 particles in previous reports [3,15]. In T2-weighted MRI images, wedge-shaped, corticosubcortical hyperintense lesions were observed in the CWS areas between the territory of the ACA and the MCA on day 10 after surgery (monkey #1 and #2). Part of these lesions showed hypointensities in the T1-weighted images, suggesting that these are CWS infarcts (Fig. 1A). In addition, multiple or confluent lesions in the IWS areas including the corona radiata and the centrum semiovale were observed. These lesions showed hypointensities in the T1-weighted images and hyperintensities in the T2-weighted images, suggesting that these are IWS infarcts (Fig. 1A). On day 71 after surgery, hyperintense spots in the T2-weighted images were reduced but some remained, and ventricular enlargement and atrophic changes were observed in the T2-weighted images (Fig. 1C). T2 star-weighted images showed multiple microbleeds near the lateral ventricle (monkey #1; Fig. 1D). The results of the MRI analysis have been summarized in Table 1. The control monkeys injected with saline showed neither microinfarcts nor atrophic changes.

In the present study, it was demonstrated that multiple microemboli can cause watershed infarcts in non-human primates. Previous reports suggest that IWS infarcts are caused mainly by hemodynamic compromise, while embolic pathogenesis contributes to the genesis of CWS infarcts [20]. However, this present study showed that IWS infarcts as well as CWS infarcts can be directly induced by embolic pathogenesis. These results may have important clinical relevance because the same report showed that IWS are frequently associated with

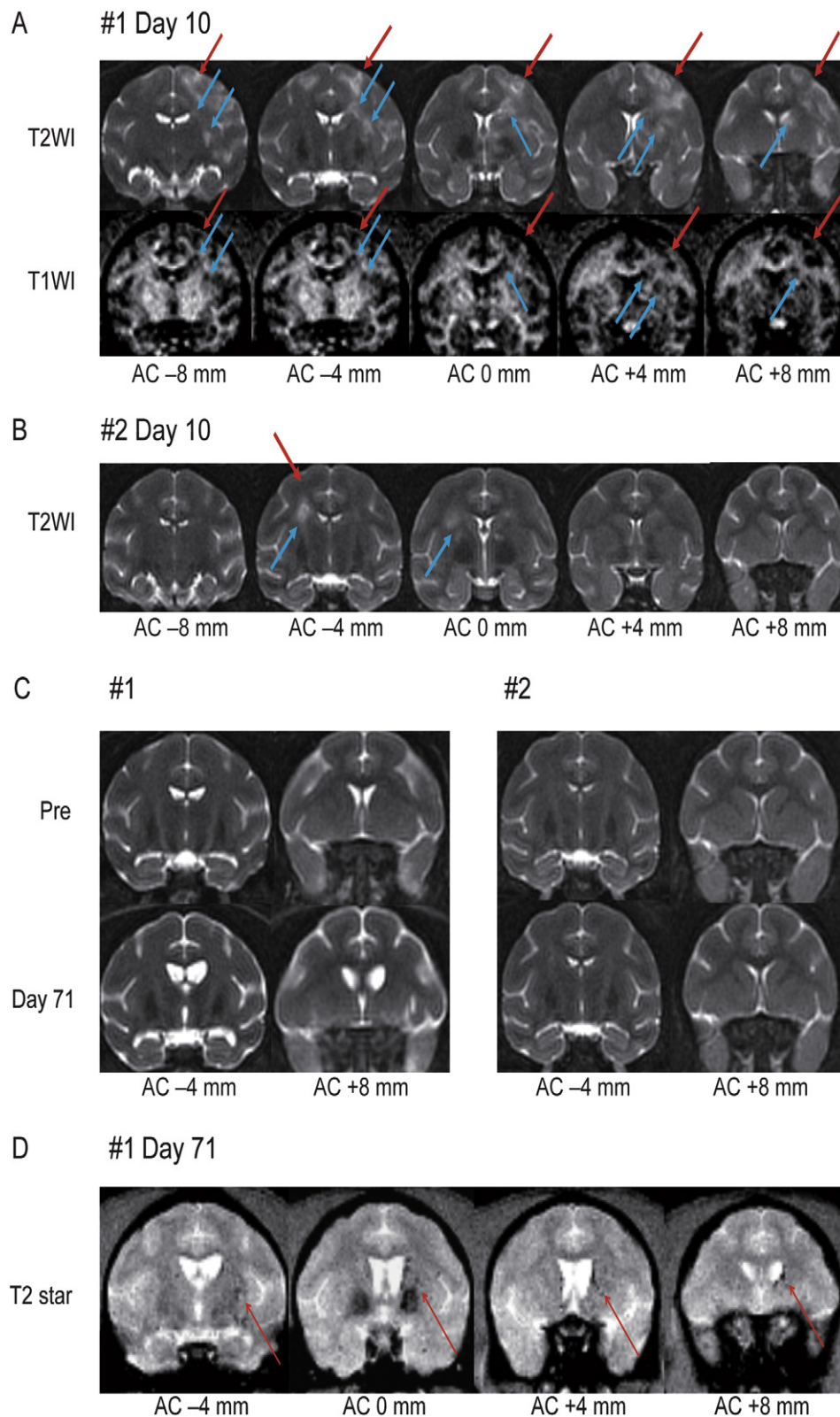


Fig. 1. Multiple microemboli cause cortical watershed (CWS) and internal watershed (IWS) infarcts in the acute phase on day 10 after the surgery and brain atrophy with microbleeds in the chronic phase on day 71 after surgery. (A–D) Serial coronal sections. Location of brain slice from each monkey was fitted at the anterior commissure (AC) as a guide. AC -8 mm indicates 8 mm posterior to AC. AC +8 mm indicates 8 mm anterior to AC. (A) T1-weighted and T2-weighted MRI images of monkey #1 on day 10 after surgery. (B) T2-weighted MRI images of monkey #2 on day 10 after surgery. Red arrows indicate CWS infarcts and blue arrows indicate IWS infarcts. (C) T2-weighted MRI images of monkey #1 and #2 at pre-operation and on day 71 after surgery. (D) T2 star-weighted MRI images of monkey #1 on day 71 after surgery. Red arrows indicate microbleeds. (For interpretation of the references to color in this figure legend, the reader is referred to the web version of the article.)

deterioration after stroke. Taken together, not only control of hemodynamic compromise, but also prevention of cerebral emboli, may decrease the risk of clinical deterioration after watershed infarcts.

The reasons why microemboli preferentially propagate to watershed areas remain unclear. The deeper brain structures within the MCA territory are supplied by long penetrating medullary arteries, which are the most distal branches of the ICA and have low perfusion pressure, and lenticulostriate arteries, which have poor collateral blood supply [18]. These anatomical characteristics may lead to the vulnerability of the IWS to hemodynamic compromise, the effect of emboli, or the synergism of both pathogenesis [2]. However, the CWS area lies in close proximity to the cortical surface, where penetrating arteries originate, meaning it receives collateral supply through leptomeningeal and dural anastomoses; this makes the CWS more resistant to decreased cerebral perfusion [20]. Caplan and Hennerici have suggested that hypoperfusion and embolism often coexist and that their pathophysiological features are interactive in borderzone infarcts [2]. In particular they proposed that impaired washout is an important concept that links hypoperfusion, embolization, and brain infarction. However, the present study showed that only embolism can cause both CWS and IWS infarcts, suggesting factors other than impaired washout, collateral blood supply, and vascular anatomy may contribute to embolic WS infarcts. In order to evaluate the mechanism of embolic WS infarcts, it would be desirable to examine how traceable microbeads, such as fluorescent microbeads, enter WS areas. Further studies are therefore warranted to clarify these issues.

Watershed infarcts in the acute phase and atrophic changes with microbleeds in the chronic phase of monkey #2 were relatively mild in comparison to monkey #1, despite the same number of microbeads being injected. Previous reports have shown that watershed infarcts are associated with a reduction in benzodiazepine receptors in the overlying cerebral cortex, suggesting that cortical neuronal damage may occur in parallel with the development of watershed infarcts [6,19]. Atrophic changes may reflect cortical neuronal damage, which occurs in parallel with development of watershed infarcts. In addition, Fisher et al. have suggested that microbleeds occur in the absence of hypertension and amyloid deposition and that both blood brain barrier (BBB) pericytes and macrophages within the neurovascular unit seem to play a role in modulating microbleeds [5]. Thus, the number of microbleeds might have been affected by the degree of BBB pericyte disruption and/or microglial activation. Furthermore, the different degrees of brain damage may result from differences in brain tissue vulnerability, white matter recovery, vascular anatomy, or embolus extravasation [8]. The elucidation of the mechanism involved in such disparity may therefore lead to the development of new therapeutic strategies for brain damage associated with embolic watershed infarcts.

The present study showed that embolic pathogenesis can directly contribute to the genesis of both CWS and IWS infarcts in a macaque monkey model of multiple microinfarcts. The recognition of embolic CWS and IWS infarcts has an important clinical relevance to prevent deterioration after stroke. Further study is needed to fully elucidate the mechanism of embolic watershed infarcts and varied brain damage caused by microemboli.

Acknowledgments

This work was conducted through the Cooperative Research Program in Tsukuba Primate Research Center, National Institute of Biomedical Innovation supported by grants from the Ministry of Health, Labor and Welfare of Japan. The authors are very grateful to the staff at the Tsukuba Primate Research Center for their excellent animal care support and to Dr. Ahmad Khundakar for his thoughtful comments.

References

- [1] J.B. Brierley, B.J. Excell, The effects of profound systemic hypotension upon the brain of *M. rhesus*: physiological and pathological observations, *Brain* 89 (1966) 269–298.
- [2] L.R. Caplan, M. Hennerici, Impaired clearance of emboli (washout) is an important link between hypoperfusion, embolism, and ischemic stroke, *Arch. Neurol.* 55 (1998) 1475–1482.
- [3] Y. Chin, Y. Sato, M. Mase, T. Kato, B. Herculano, M. Sekino, H. Ohsaki, N. Ageyama, F. Ono, K. Terao, Y. Yoshikawa, T. Hisatsune, Transient decrease in cerebral motor pathway fractional anisotropy after focal ischemic stroke in monkey, *Neurosci. Res.* 66 (2010) 406–411.
- [4] M. Del Sette, M. Eliasziw, J.Y. Streifler, V.C. Hachinski, A.J. Fox, H.J. Barnett, Internal borderzone infarction: a marker for severe stenosis in patients with symptomatic internal carotid artery disease. For the North American Symptomatic Carotid Endarterectomy (NASCET) Group, *Stroke* 31 (2000) 631–636.
- [5] M. Fisher, S. French, P. Ji, R.C. Kim, Cerebral microbleeds in the elderly: a pathological analysis, *Stroke* 41 (2010) 2782–2785.
- [6] C. Giffard, B. Landeau, N. Kerrouche, A.R. Young, L. Barre, J.C. Baron, Decreased chronic-stage cortical 11C-flumazenil binding after focal ischemia–reperfusion in baboons: a marker of selective neuronal loss? *Stroke* 39 (2008) 991–999.
- [7] S. Honjo, The Japanese Tsukuba Primate Center for Medical Science (TPC): an outline, *J. Med. Primatol.* 14 (1985) 75–89.
- [8] C.K. Lam, T. Yoo, B. Hiner, Z. Liu, J. Grutzendler, Embolus extravasation is an alternative mechanism for cerebral microvascular recanalization, *Nature* 465 (2010) 478–482.
- [9] R. Leblanc, Y.L. Yamamoto, J.L. Tyler, M. Diksic, A. Hakim, Borderzone ischemia, *Ann. Neurol.* 22 (1987) 707–713.
- [10] J. Masuda, C. Yutani, J. Ogata, Y. Kuriyama, T. Yamaguchi, Atheromatous embolism in the brain: a clinicopathologic analysis of 15 autopsy cases, *Neurology* 44 (1994) 1231–1237.
- [11] I. Momjian-Mayor, J.C. Baron, The pathophysiology of watershed infarction in internal carotid artery disease: review of cerebral perfusion studies, *Stroke* 36 (2005) 567–577.
- [12] R.R. Moustafa, D. Izquierdo-Garcia, P.S. Jones, M.J. Graves, T.D. Fryer, J.H. Gillard, E.A. Warburton, J.C. Baron, Watershed infarcts in transient ischemic attack/minor stroke with > or =50% carotid stenosis: hemodynamic or embolic? *Stroke* 41 (2010) 1410–1416.
- [13] M. Mull, M. Schwarz, A. Thron, Cerebral hemispheric low-flow infarcts in arterial occlusive disease. Lesion patterns and angiomorphological conditions, *Stroke* 28 (1997) 118–123.
- [14] M.S. Pollanen, J.H. Deck, The mechanism of embolic watershed infarction: experimental studies, *Can. J. Neurol. Sci.* 17 (1990) 395–398.
- [15] Y. Sato, Y. Chin, T. Kato, Y. Tanaka, Y. Tozuka, M. Mase, N. Ageyama, F. Ono, K. Terao, Y. Yoshikawa, T. Hisatsune, White matter activated glial cells produce BDNF in a stroke model of monkeys, *Neurosci. Res.* 65 (2009) 71–78.
- [16] S.I. Savitz, M. Fisher, Future of neuroprotection for acute stroke: in the aftermath of the SAINT trials, *Ann. Neurol.* 61 (2007) 396–402.
- [17] K.S. Wong, S. Gao, Y.L. Chan, T. Hansberg, W.W. Lam, D.W. Droste, R. Kay, E.B. Ringelstein, Mechanisms of acute cerebral infarctions in patients with middle cerebral artery stenosis: a diffusion-weighted imaging and microemboli monitoring study, *Ann. Neurol.* 52 (2002) 74–81.
- [18] H. Yamauchi, H. Fukuyama, J. Kimura, J. Konishi, M. Kameyama, Hemodynamics in internal carotid artery occlusion examined by positron emission tomography, *Stroke* 21 (1990) 1400–1406.
- [19] H. Yamauchi, R. Nishii, T. Higashi, S. Kagawa, H. Fukuyama, Hemodynamic compromise as a cause of internal border-zone infarction and cortical neuronal damage in atherosclerotic middle cerebral artery disease, *Stroke* 40 (2009) 3730–3735.
- [20] S.W. Yong, O.Y. Bang, P.H. Lee, W.Y. Li, Internal and cortical border-zone infarction: clinical and diffusion-weighted imaging features, *Stroke* 37 (2006) 841–846.